



## A modern pollen dataset from lake surface sediments on the central-western Tibetan Plateau

Qingfeng Ma<sup>1</sup>, Liping Zhu<sup>1,2</sup>, Jianting Ju<sup>1</sup>, Junbo Wang<sup>1</sup>, Yong Wang<sup>3</sup>, Lei Huang<sup>4</sup>, Torsten Haberzettl<sup>5</sup>

<sup>1</sup>State Key Laboratory of Tibetan Plateau Earth System, Environment and Resources (TPESER), Institute of Tibetan Plateau Research, Chinese Academy of Sciences, Beijing, 100101, China

<sup>2</sup>University of Chinese Academy of Sciences, Beijing, 100049, China

<sup>3</sup>Anhui Key Laboratory of Earth Surface Processes and Regional Response in Yangtze-Huaihe River Basin, School of Geography and Tourism, Anhui Normal University, Wuhu, 241002, China

<sup>4</sup>College of Resource Environment and Tourism, Capital Normal University, Beijing, 100048, China

<sup>5</sup>Physical Geography, Institute for Geography and Geology, University of Greifswald, Greifswald, 17489, Germany

**Correspondence:** Liping Zhu ([lpzhu@itpcas.ac.cn](mailto:lpzhu@itpcas.ac.cn))

15

20



**Abstract.** Modern pollen datasets are essential for pollen-based quantitative paleoclimate (e.g. precipitation) reconstructions, which can aid to better understand recent climate change and its underlying forcing mechanisms. A modern pollen dataset based on surface sediments from 90 lakes in the shrub, meadow, steppe and desert regions of the central and western Tibetan Plateau (TP) was established to fill geographical gaps left by previous datasets. Ordination analyses of pollen data and climatic parameters revealed that annual precipitation is the dominant factor for modern pollen distribution on the central and western TP. A regional transfer function for annual precipitation was developed with the weighted averaging partial least squares (WAPLS), which suggests a good inference power of the modern pollen dataset for annual precipitation. A case study in which the transfer function was effectively applied to a fossil pollen record from Lake Tangra Yumco on the central TP for paleoprecipitation reconstruction demonstrated the significance of the modern pollen dataset in less data region for paleoclimate change studies. Data from this study are openly available via the Zenodo portal (Ma et al., 2023; <https://doi.org/10.5281/zenodo.8008474>).

## 1 Introduction

Quantitative reconstructions of climate data beyond the range of the instrumental record are required to understand climate change at global and regional scales (Nakagawa et al., 2002; Lu et al., 2011), and to identify the underlying forcing mechanisms of climate change. Pollen extracted from lake sediment sequences has frequently been used to quantitatively reconstruct paleoclimate at different scales from continental, regional to site-specific (Seppä et al., 2004; Lu et al., 2011). Available pollen-climate calibration sets consist of modern pollen data and the corresponding climate data. Modern pollen data from different sources (topsoils, moss pollsters, peat bogs and lake sediments) in one region have different relevant pollen source areas and taphonomy (Wilmshurst and McGlone, 2005; Zhao et al., 2009; Birks et al., 2010). Therefore, for quantitative paleoclimate reconstructions based on fossil pollen in lake sediment records, modern pollen data for the calibration set should be extracted preferably from lake surface sediments if possible to ensure a high comparable quality (Birks et al., 2010).

The Tibetan Plateau (TP), known as the “Third Pole” of the Earth, covers a vast geographical area with an average elevation of more than 4000 m a.s.l. (Yao et al., 2013). Due to its large-scale climatic influence, sensitivity to climate change, and weak degree of anthropogenic influence, the TP has become a key region to study present and past climate change and the underlying forcing mechanisms. To date, there are several modern pollen datasets from the TP that have been used to develop the pollen-climate calibration sets (Shen et al., 2006; Herzsuh et al., 2010; Lu et al., 2011; Cao et al., 2021). However, these datasets are mostly from the eastern TP, desperately short of samples from lake surface sediments evenly distributed across the central and western TP. A large number of evenly distributed lakes from the central and western TP provide an opportunity to establish a lake surface sediment pollen dataset for this region.

Here we present and analyse a modern pollen dataset from lake surface sediments on the central and western TP. Our aims are to (1) describe the modern pollen assemblages on the central and western TP; (2) determine the key climatic variable that is mainly responsible for controlling the pollen distribution on the central and western TP; (3) derive a regional



pollen-climate transfer function to be able to quantitatively reconstruct the key climatic variable; (4) evaluate the predictive power of our pollen dataset for quantitative paleoclimate reconstruction through a case study. This modern pollen dataset not only supports the accurate regional paleoclimate reconstruction in the central and western TP, but also fills a geographical gap left by previous datasets to improve the reliability of quantitative climate reconstructions for the entire TP.

## 2 Study area

### 2.1 Climate

The study area is located on the central and western TP between 28.5°–35.2° N and 79.8°–91.5° E. Altitudes of the lakes sampled for surface sediment range from 4240 to 5220 m a.s.l. (Table 1). The average elevation of these lakes is 4740 m a.s.l. The area is influenced by the Indian summer monsoon in summer and the Westerlies in winter (Yao et al., 2013). The region spans over several climatic zones from the frigid arid climate zone in the northwest to the temperate arid climate zone in the west part, to the subfrigid semi-arid climate zone in the central and north, and the temperate semi-arid climate zone in the south (Institute of Geography, 1990). The study area is characterized by cool-humid summers and cold-dry winters with mean annual temperatures between -13 and 5 °C and a mean annual precipitation of 50-500 mm from 1981 to 2010 (Figure 1a; He et al., 2020).

**Table 1.** Summary statistics of environmental parameters in the pollen dataset.

Climate variable	Minimum	Maximum	Mean	Standard deviation
Altitude (m a.s.l.)	4241	5217	4740	243
$P_{\text{ann}}$ (mm)	75	478	236	109
$T_{\text{ann}}$ (°C)	-13	4.2	-3.4	4.1
$T_{\text{July}}$ (°C)	0.4	13.4	7.8	3.3
$T_{\text{Jan}}$ (°C)	-26.3	-4	-14.7	5.1

### 2.2 Vegetation

Vegetation mainly consists of shrubs, meadows, steppes and deserts (Figure 1b; ITCAS, 1988; Institute of Geography, 1990; Hou, 2001). Shrubs, generally including *Sophora*, *Ceratostigma*, *Rosa*, *Caragana*, *Rhododendron*, *Potentilla*, and *Berberis*, are mainly distributed below 4800 m a.s.l. in the southern part of the study area. Alpine meadows are mainly found at an elevation of 4500-5300 m a.s.l. in the eastern part, at 4700-5200 m a.s.l. in the south, and 5100-5300 m a.s.l. in the central-southern part. They mainly consist mainly of *Kobresia pygmaea* communities, associated with plants of *Kobresia*, *Carex*, Poaceae, *Stipa*, Asteraceae, Ranunculaceae, Polygonaceae, and Fabaceae. Alpine steppes occupy the greatest part of the study area, which are distributed at 5100-5400 m a.s.l. in the northwestern part and below 5100 m a.s.l. in other parts. The composition of family and genus in the Tibetan steppe is dominated by Poaceae (e.g., *Stipa spp.*) and Asteraceae (e.g. *Artemisia spp.*), together with Cyperaceae, Fabaceae, Caryophyllaceae, Brassicaceae and Amaranthaceae (formerly known



as Chenopodiaceae, classified into the family Amaranthaceae). Alpine deserts are mainly distributed in the west and northwest (4200-5100 m a.s.l.). The plant communities are dominated by Amaranthaceae and Asteraceae, such as *Ceratoides latens*, *C. compacta*, *Ajania fruticulosa* and *Artemisia sp.*, together with Poaceae, Fabaceae, Brassicaceae, and *Ephedra* (ITCAS, 1988; Institute of Geography, 1990; Hou, 2001).

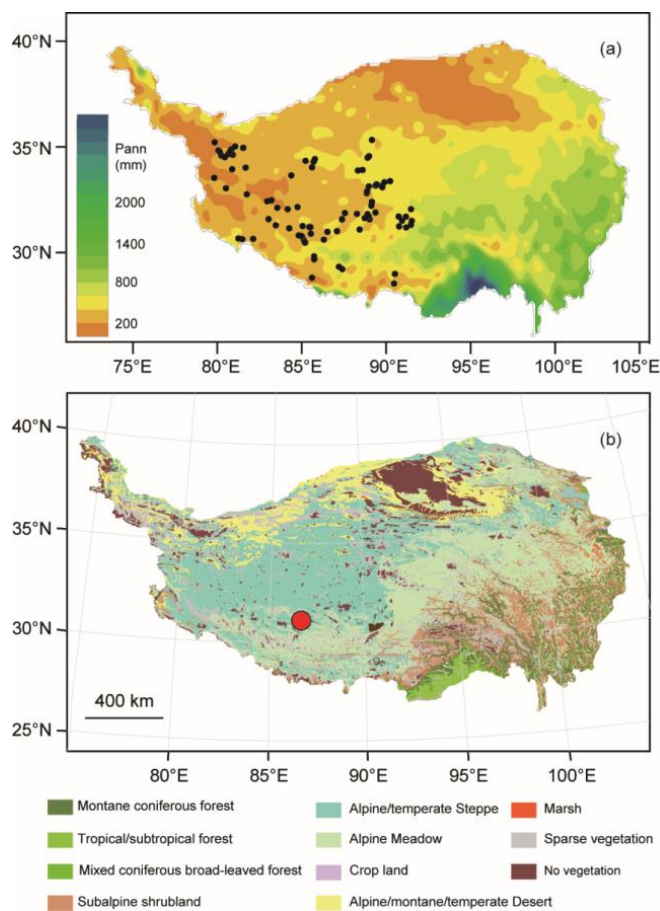


**Figure 1.** Study area and sampling sites of modern lake sediments. (a) Spatial distributions of sampling lake sites (black dots) and annual precipitation and (b) vegetation map of the Tibetan Plateau with the location of Lake Tangra Yumco (red dot).

### 3 Materials and Methods

#### 3.1 Pollen sample collection and analysis

Lake surface sediments were collected from 90 lakes in the study area, including the previously studied 31 lake surface sediment samples (Ma et al., 2017). These lakes fill the geographical gaps in the central and western TP, especially the northern Tibet, where is difficult to access due to the lack of the settlements and roads (Figure 1a). To reduce the influence of the lakeshore vegetation on the pollen spectra, surface sediments were sampled from the central part of each lake. The top 2 cm of sediment was collected as a single sample for each lake, corresponding approximately to the deposition of the last



10-20 years (Wang et al., 2020). Approximately 5 g (dry weight) of each sample was subsampled and used for pollen extraction. Samples were prepared using standard techniques (Fægri and Iversen, 1975), involving 10% HCl, 10% KOH, 40% HF, and a mixture (9:1) of acetic anhydride and sulfuric acid, followed by sieving through a 10 µm mesh. Pollen identification and counting were performed under a ZEISS microscope at 400× magnification, aided by published keys (Tang et al., 2017; Wang et al., 1995). More than 300 pollen grains were counted for each sample. A total of 70 pollen taxa were recognized from the surface sediments of 90 lakes (Table 2).

### 3.2 Climate parameter processing

Climate data were obtained from the Chinese Meteorological Forcing Dataset (He et al., 2020). The dataset is based on the fusion of remote sensing products, reanalysis datasets and in-situ station data, with a temporal resolution of 3 hours and a spatial resolution of 0.1 °. The dataset has been positively validated for western China where observational data are sparse. Near-surface (2 m) air temperature and precipitation rates were extracted for each lake during 1981-2010 based on their longitude and latitude. These were subsequently transformed to mean annual temperature ( $T_{ann}$ ), mean July temperature ( $T_{July}$ ), mean January temperature ( $T_{Jan}$ ) and mean annual precipitation ( $P_{ann}$ ) to estimate the influence of climate variables on modern pollen distribution. The four climate variables were selected because they are important limiting factors for pollen distribution and plant growth, are commonly presented in climate models, and are most relevant for paleoclimatic reconstructions (Lu et al., 2011; Cao et al., 2021). Summary statistics for the four climate variables are presented in Table 1.

**Table 2.** List of the 70 pollen taxa in the modern dataset, derived from lake surface sediments (SD= Standard deviation).

Pollen taxa	Hill's N2	Min.	Max.	Mean	SD	Pollen taxa	Hill's N2	Min.	Max.	Mean	SD
<i>Picea</i>	28.80	0.00	2.90	0.36	0.52	<i>Aster</i>	43.68	0.00	7.15	1.37	1.41
<i>Abies</i>	12.87	0.00	1.69	0.11	0.27	<i>Pedicularis</i>	17.03	0.00	1.10	0.11	0.22
<i>Pinus</i>	61.67	0.31	36.60	10.74	7.28	Caryophyllaceae	32.91	0.00	10.80	1.15	1.51
<i>Tsuga</i>	23.16	0.00	4.75	0.42	0.73	<i>Humulus</i>	13.91	0.00	1.33	0.10	0.24
<i>Cedrus</i>	23.67	0.00	1.36	0.16	0.27	Rosaceae	44.91	0.00	17.42	3.52	3.52
<i>Keteleeria</i>	9.65	0.00	0.94	0.06	0.17	Brassicaceae	44.80	0.00	4.17	0.81	0.82
<i>Betula</i>	43.71	0.00	9.86	1.55	1.60	Amaranthaceae	34.09	0.00	64.60	11.59	14.84
<i>Alnus</i>	25.65	0.00	8.86	0.94	1.49	Zygophyllaceae	12.09	0.00	1.21	0.08	0.19
<i>Ulmus</i>	8.67	0.00	1.30	0.07	0.21	Cyperaceae	58.46	1.62	88.18	23.58	17.32
<i>Quercus E</i>	38.56	0.00	9.68	1.61	1.86	Lamiaceae	15.74	0.00	8.70	0.45	0.98
<i>Corylus</i>	1.00	0.00	0.76	0.01	0.08	<i>Thalictrum</i>	35.41	0.00	3.78	0.49	0.61
<i>Carpinus</i>	11.04	0.00	3.00	0.19	0.50	Ranunculaceae	35.78	0.00	5.90	0.97	1.19
<i>Cyclobalanopsis</i>	1.00	0.00	0.33	0.01	0.03	<i>Saxifraga</i>	14.38	0.00	1.92	0.20	0.45
<i>Quercus D</i>	12.69	0.00	3.26	0.22	0.53	<i>Gentiana</i>	6.69	0.00	6.41	0.22	0.79
<i>Pterocarya</i>	3.99	0.00	0.32	0.01	0.06	<i>Polygonum</i>	30.53	0.00	1.92	0.32	0.45
<i>Juglans</i>	16.36	0.00	0.56	0.06	0.13	<i>Taraxacum</i>	13.41	0.00	2.24	0.16	0.37
<i>Rhamnus</i>	3.28	0.00	0.72	0.02	0.10	Apiaceae	6.57	0.00	0.82	0.04	0.14



Moraceae	1.98	0.00	0.31	0.01	0.04	Euphorbiaceae	12.51	0.00	6.65	0.39	0.97
Celastraceae	1.00	0.00	0.31	0.00	0.03	Solanaceae	2.68	0.00	0.84	0.02	0.13
Theaceae	1.00	0.00	0.20	0.00	0.02	Boraginaceae	1.00	0.00	0.32	0.00	0.03
<i>Rhus</i>	1.00	0.00	0.30	0.00	0.03	<i>Urtica</i>	3.76	0.00	3.27	0.08	0.36
<i>Acer</i>	1.00	0.00	0.32	0.00	0.03	<i>Peganum</i>	2.75	0.00	0.65	0.02	0.10
Symplocaceae	1.00	0.00	0.33	0.00	0.03	Thymelaeaceae	3.54	0.00	0.67	0.02	0.10
<i>Salix</i>	7.64	0.00	0.49	0.03	0.09	<i>Stellera</i>	1.00	0.00	0.29	0.00	0.03
Ericaceae	8.84	0.00	0.31	0.03	0.08	<i>Rumex</i>	8.04	0.00	0.69	0.04	0.11
<i>Spiraea</i>	6.29	0.00	0.90	0.04	0.14	Scrophulariaceae	3.71	0.00	0.54	0.02	0.08
<i>Ephedra</i>	25.89	0.00	4.86	0.51	0.80	<i>Sanguisorba</i>	1.99	0.00	0.35	0.01	0.05
<i>Tamarix</i>	4.87	0.00	1.20	0.04	0.16	Rubiaceae	7.97	0.00	3.00	0.13	0.41
<i>Hippophae</i>	29.06	0.00	7.97	0.68	0.98	Liliaceae	4.00	0.00	0.30	0.01	0.06
<i>Nitraria</i>	15.86	0.00	2.00	0.15	0.33	Crassulaceae	2.97	0.00	0.30	0.01	0.05
<i>Elaeagnus</i>	2.42	0.00	1.49	0.03	0.17	Primulaceae	1.00	0.00	0.32	0.00	0.03
Fabaceae	31.22	0.00	2.58	0.40	0.55	<i>Erigeron</i>	5.35	0.00	0.60	0.02	0.09
<i>Artemisia</i>	69.65	1.29	66.67	29.28	15.82	Haloragaceae	1.00	0.00	0.31	0.00	0.03
Poaceae	51.77	0.00	25.56	5.00	4.29	Typhaceae	1.69	0.00	0.72	0.01	0.08
Asteraceae	39.16	0.00	9.20	1.37	1.56	<i>Potamogeton</i>	1.95	0.00	1.29	0.02	0.17

### 3.3 Numerical analyses

115 Ordination techniques were used to identify co-varying patterns between modern pollen spectra and environmental variables. In order to stabilize the variances and to optimize the signal-to-noise ratio in the dataset, pollen percentages were square-root-transformed (Prentice, 1980). Detrended correspondence analysis (DCA) was used to determine which method (e.g. linear or non-linear method) was most suitable based on gradient length as the criterion. The DCA result showed that pollen data have a gradient length of 2.2 standard deviations. Therefore, a linear method (redundancy analysis (RDA)) was considered appropriate for our pollen data. An RDA was carried out to detect the influence of climate variables on our modern pollen dataset. Monte Carlo permutation tests (999 unrestricted permutations) were used to assess the statistical significance of the RDA models. To reduce the bias caused by the effects of high collinearity between climate variables in the ordination analysis process, we examined the variance inflation factors (VIFs) for each variable. If the VIF value of a variable was larger than 20, the variable was expected to be collinear with other variables and to capture little variance. The initial RDA showed that the VIF values of the variables  $T_{\text{ann}}$ ,  $T_{\text{Jan}}$  and  $T_{\text{July}}$  were greater than 20. However, after deleting  $T_{\text{ann}}$  that held the highest VIF value, the remaining three climate variables had VIF values lower than 20 and could therefore be used in the final RDA to discern their influence on the modern pollen dataset. These analyses were performed using the Canoco 5 software (ter Braak and Smilauer, 2012).

To assess the potential of the modern pollen dataset for quantitative estimates of climate parameters, the Weighted Averaging Partial Least Squares (WAPLS) model was run. WAPLS is one of the most robust techniques for numerical



climate inference (ter Braak and Juggins, 1993) and has been widely used in quantitative analyses of relationships between biological assemblages and environmental factors on the TP, such as on pollen (Shen et al., 2006; Herzschuh et al., 2010) and other proxy data, e.g. chironomid (Zhang et al., 2019). Error estimates of the WAPLS model were compared with other calibration models, including weighted averaging (WA) regression with inverse deshrinking (Birks et al., 1990) and the  
135 Modern Analogue Technique (MAT) (Overpeck et al., 1985). The optimal model is chosen which produces a high coefficient of determination ( $R^2$ ) between observed and predicted values, a low root mean square error of prediction (RMSEP) and a low maximum bias. In addition to the traditional leave-one-out cross-validation, a novel method (Telford and Birks, 2011) was used to assess the statistical significance of the climate reconstruction using the statistical package R 4.2.3 (R Core Team, 2023) with the *randomTF* function in the *palaeoSig* package 2.1-3 (Telford and Trachsel, 2023). Model  
140 development and climate reconstructions were performed in the C2 software (Juggins, 2003).

To evaluate the inference power of our pollen dataset for paleoclimatic parameters, an application of the WAPLS model to the Lake Tangra Yumco fossil pollen record (covering the last 17.5 cal kyr BP; Ma et al., 2019, 2020) was made to quantitatively estimate the last deglacial and Holocene paleoclimate in the south-central part of the TP. Lake Tangra Yumco (31.2°N, 86.7°E, 4545 m a.s.l.) is located in the semi-arid region, and its catchment is mainly occupied by alpine steppe  
145 (Figure 1b).

#### 4 Pollen data and relations to climate factors

The pollen assemblages in the surface sediments of the 90 lakes, consisting of a total of 70 pollen taxa, are summarized in Table 1. The pollen assemblages (Figure 2) are dominated by herbaceous taxa, especially *Artemisia* (mean  $29.3 \pm 15.8\%$ , max. 66.7%), Cyperaceae (mean  $23.6 \pm 17.3\%$ , max. 88.2%) and Amaranthaceae (mean  $11.6 \pm 14.8\%$ , max. 64.6%). The  
150 sum percentage of these three taxa is up to 64.4%. Other common herbaceous pollen taxa include Poaceae (mean  $5 \pm 4.3\%$ , max. 25.6%), *Aster* (mean  $1.4 \pm 1.4\%$ , max. 7.2%), Asteraceae (mean  $1.4 \pm 1.6\%$ , max. 9.2%), Caryophyllaceae (mean  $1.2 \pm 1.5\%$ , max. 10.8%), Ranunculaceae (mean  $1.0 \pm 1.2\%$ , max. 5.9%), Brassicaceae (mean  $0.8 \pm 0.8\%$ , max. 4.2%), and *Thalictrum* (mean  $0.5 \pm 0.6\%$ , max. 3.8%). Tree pollen consists mainly of *Pinus* (mean  $10.7 \pm 7.3\%$ , max. 36.6%), *Quercus*-evergreen (mean  $1.6 \pm 1.9\%$ , max. 9.7%), *Betula* (mean  $1.6 \pm 1.6\%$ , max. 9.9%) and *Alnus* (mean  $1.0 \pm 1.5\%$ , max. 8.9%).  
155 Shrub pollen percentages are low, mainly consisting of Rosaceae (mean  $3.5 \pm 3.5\%$ , max. 17.4%), *Hippophae* (mean  $0.7 \pm 1.0\%$ , max. 8.0%) and *Ephedra* (mean  $0.5 \pm 0.8\%$ , max. 4.9%).

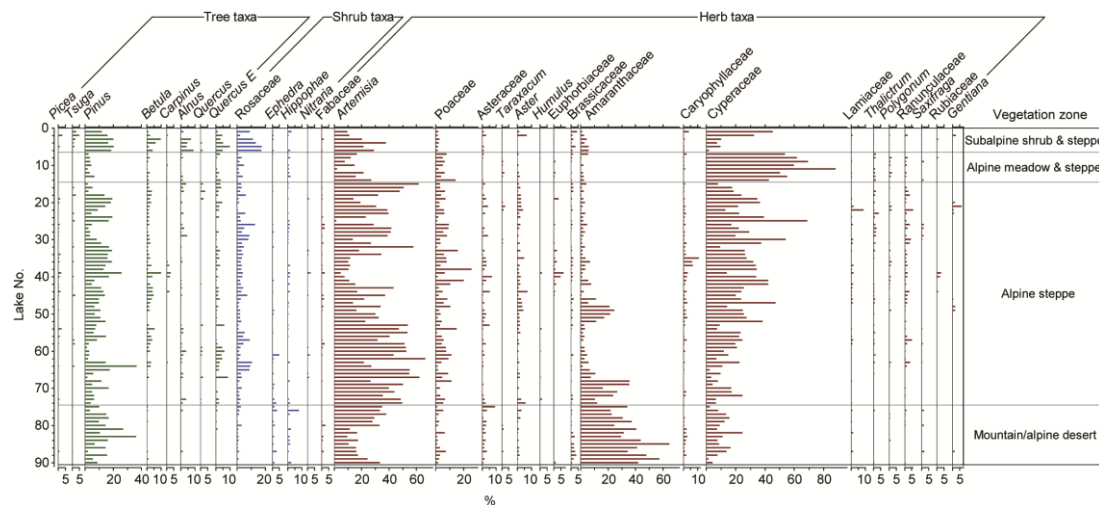


**Figure 2.** Pollen diagram for lake surface sediments from the central and western Tibetan Plateau showing the percentage values of selected pollen taxa. The samples are arranged according to their vegetation zones.

160 A series of RDAs based on 31 pollen taxa (1% in at least two samples) and three climatic variables ( $P_{ann}$ ,  $T_{Jan}$  and  $T_{July}$ ) show that  $P_{ann}$ , as a sole variable, explains 24.2% of the variation in the pollen data, which is significantly more than the explained proportion of  $T_{Jan}$  (8.6%) and  $T_{July}$  (2.5%). The RDA result with all climatic variables is shown in Figure 3. RDA axis 1 and axis 2 capture 26.5% and 7.2% of the variation in the pollen data, respectively. Humid-preferring taxa including Cyperaceae, *Thalictrum*, Ranunculaceae, and *Polygonum* are located along the positive direction of  $P_{ann}$ , whereas arid-  
 165 preferring taxa consisting of Amaranthaceae, *Ephedra*, *Artemisia*, and Asteraceae are distributed along the negative direction of  $P_{ann}$ . Tree pollen taxa are mainly located along the positive direction of  $T_{Jan}$  and  $T_{July}$ .

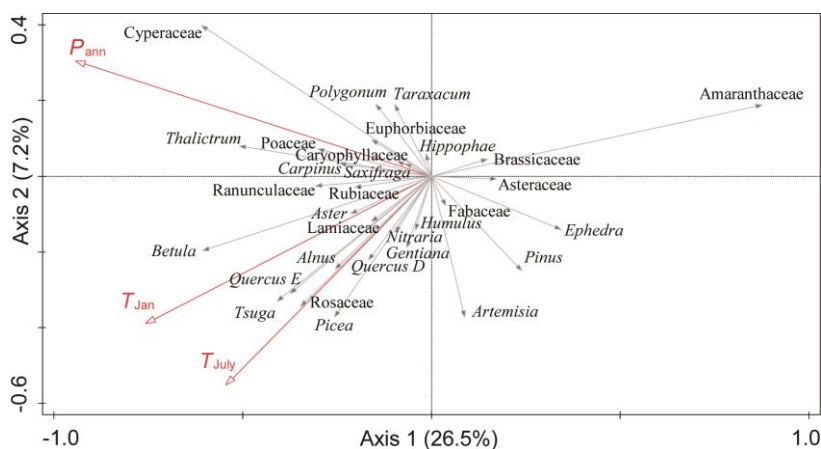


**Figure 3.** Redundancy analysis (RDA) results for the main pollen taxa in the surface lake sediments and three important climatic variables ( $P_{ann}$  = mean annual precipitation;  $T_{Jan}$  = January temperature;  $T_{July}$  = July temperature).  
 170



## 5 Pollen-climate transfer function construction and application

RDA results indicate that  $P_{\text{ann}}$  is the leading climate variable for modern pollen distribution in the central and western TP (Figure 3; Table 3). The associated Monte Carlo permutation test exhibits that the relationship between pollen taxa and  $P_{\text{ann}}$  is significant ( $p = 0.001$ ) (Table 3). Thus, the numerical relationship between modern  $P_{\text{ann}}$  and pollen assemblages shows that the pollen dataset has robust ability to infer the changes in climatic variables. According to the error estimates for several calibration models, the WAPLS component 2 shows a better performance than WA, WAT and WAPLS component 1, due to its highest  $R^2$ , the lowest RMSEP, and the lowest maximum bias (Table 4). WAPLS component 2 yields a reduction of more than 5% in RMSEP relative to component 1, which is a ‘useful’ component (Birks, 1998). For the WAPLS component 2 model, the residual between the observed and predicted  $P_{\text{ann}}$  of Lake 3 exceeds 2.5 standard deviations, which is thus regarded as an outlier. Finally, after removing the pollen dataset, the WAPLS approach was employed to develop the pollen-climate transfer function.

**Table 3.** Summary statistics of redundancy analysis (RDA) based on main pollen taxa and four climate variables. VIF is the variance inflation factor (without  $T_{\text{ann}}$ ). Variance explained (%) is the proportion of variation in the pollen assemblages explained by each variable as the sole constraining variable in RDA.  $p$  value indicates the statistical significance of each variable assessed by Monte Carlo permutation tests (999 unrestricted permutations).

Climate variable	VIF	Variance explained (%)	$p$
$P_{\text{ann}}$	3.7	24.2	0.001
$T_{\text{Jan}}$	11.1	8.6	0.001
$T_{\text{July}}$	6.6	2.5	0.002
$T_{\text{ann}}$	–	–	–

**Table 4.** Error estimates for different  $P_{\text{ann}}$  calibration models, assessed by leave-one-out cross-validation in terms of coefficient of determination between predicted and observed  $P_{\text{ann}}$ , the maximum bias (Max. bias) (mm), root mean square error of prediction (RMSEP) (mm), and a reduction of RMSEP in WAPLS components.

Method	$R^2$	Max. bias (mm)	RMSEP (mm)	%Change
WA_inv	0.69	131.5	65.8	
MAT	0.63	153.3	67	
WMAT	0.64	151.6	66.3	
WAPLS1	0.72	122.1	62	
WAPLS2	0.81	65.6	56.1	9.6



190 The final WAPLS component 2 model shows a good performance ( $R^2 = 0.81$ , RMSEP = 56.1 mm, maximum bias = 65.6 mm). The results of the WAPLS component 2 model for  $P_{\text{ann}}$  with a plot of predicted versus observed values are shown in Figure 4. The results indicate that WAPLS component 2 performs well for  $P_{\text{ann}}$  inference. However, the plot of the residuals versus  $P_{\text{ann}}$  values shows an underestimate for humid sites ( $P_{\text{ann}} > 400$  mm). Nevertheless, quantitative reconstructions covering the arid and semi-arid region of the TP ( $P_{\text{ann}} < 400$  mm) should be credible due to the low bias.

195

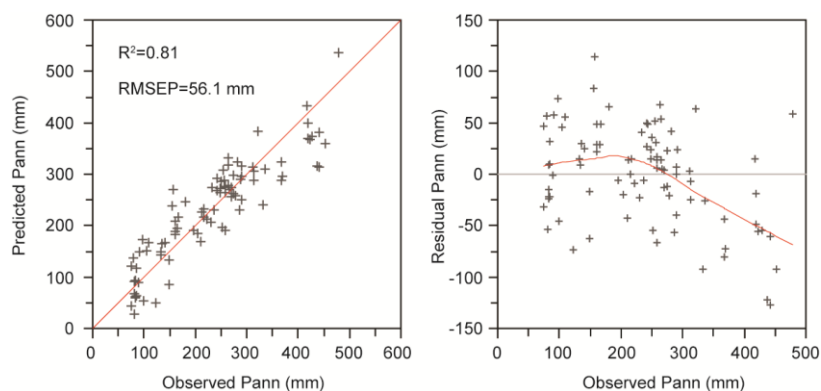
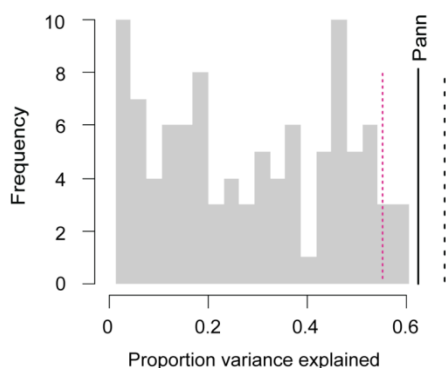


**Figure 4.** Scatter plots of WAPLS inference model for observed annual precipitation (Pann) vs. predicted Pann values (left) and residuals vs. Pann values (right).

Fossil pollen assemblages and concentrations from Lake Tangra Yumco revealed that the desert vegetation was replaced by steppe vegetation during the last deglaciation, and alpine steppe persisted in the basin during the Holocene (Ma et al., 2019, 2020). The results indicated that arid or semi-arid climatic condition persisted since 17.5 cal kyr BP. Therefore, the regional transfer function for  $P_{\text{ann}}$  can be used for this record. Statistical significance tests showed that the  $P_{\text{ann}}$  reconstruction for Lake Tangra Yumco explained more of the variance in the fossil data than 95% of the reconstructions from transfer functions trained on random data. The proportion of the variance explained by the  $P_{\text{ann}}$  reconstruction was also closer to that explained by the first axis of principal component analysis (PCA) which represented the maximum proportion of the variance in the fossil pollen data that the reconstruction could possibly explain (Telford and Birks, 2011). The above results indicate that the  $P_{\text{ann}}$  reconstruction for Lake Tangra Yumco is statistically significant, and the reconstruction is reliable using the WAPLS model (Figure 5).

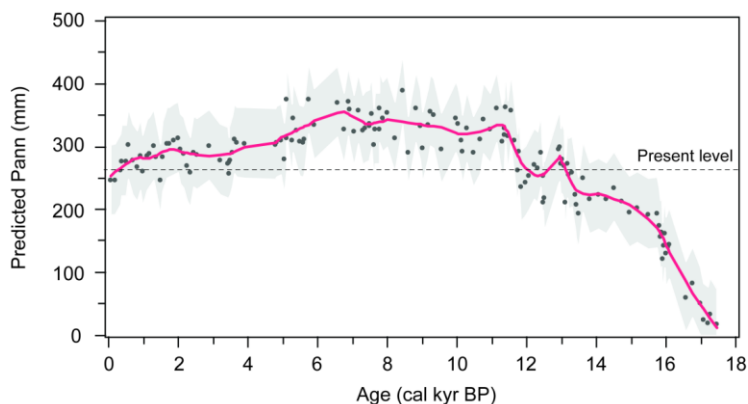
200

205



210 **Figure 5.** Statistical significance test of Pann reconstruction for Lake Tangra Yumco. Histogram showing the proportion of  
the variance in the pollen record of Lake Tangra Yumco explained by reconstructions of 99  $P_{ann}$  calibration functions trained  
with random data. The dotted red line represents the proportion of variance explained by random data-trained calibration  
functions at the 95% confidence level. The black solid line indicates the proportion of variance explained by the  
reconstructed  $P_{ann}$ . The dotted black line marks the proportion of variance explained by the first axis of the principal  
215 component analysis (PCA).

The application of the WAPLS transfer function for  $P_{ann}$  to the Lake Tangra Yumco pollen data is the first quantitative  
record in the central-western TP, located in the Indian summer monsoon margin. To ensure the effective number of species  
occurrences and uniformity, predicted  $P_{ann}$  values for fossil samples with Hill's  $N_2 > 4$  (Hill, 1973) were used in the  
reconstruction result (Figure 6). The pollen-derived precipitation record shows that the lake basin was most arid from 17.5 to  
220 16.1 cal kyr BP with  $< 100$  mm of  $P_{ann}$ . During 16.1-13.2 cal kyr BP,  $P_{ann}$  increased rapidly up to  $> 200$  mm.  $P_{ann}$  showed a  
peak value (up to 300 mm) at approximately 13 cal kyr BP, followed by a low value of 240 mm at approximately 12 cal kyr  
BP.  $P_{ann}$  was highest values in the early and middle Holocene (11.6-5 cal kyr BP), which is 80 mm (30%) higher than  
modern annual precipitation. After 5 cal kyr BP,  $P_{ann}$  showed a decreasing trend.



225 **Figure 6.** Predicted annual precipitation (Pann) for Lake Tangra Yumco using the weighted averaging partial least squares  
(WAPLS) inference model. The dotted line represents the modern annual precipitation of the basin. Grey shading indicates



the ranges from predicted values subtracting the root mean square error of prediction (RMSEP) to predicted values adding the RMSEP.

## 6 Data availability

230 The dataset includes pollen counts and pollen percentages of the lake surface samples. Locations (latitude, longitude and altitude) and climatic data for each lake site are also given in the dataset. This dataset can be openly accessible via Zenodo portal: <https://doi.org/10.5281/zenodo.8008474> (Ma et al., 2023).

## 7 Summary

We present and analyse a pollen dataset based on surface sediments from 90 lakes covering the central-western TP. This dataset includes pollen counts and percentages, as well as latitude, longitude, altitude and corresponding climate data. Ordination analyses indicate that mean annual precipitation ( $P_{\text{ann}}$ ) is the dominant climatic parameter controlling variations in the modern pollen distribution of the dataset on the central-western TP. A quantitative transfer function was developed to estimate  $P_{\text{ann}}$  from the modern pollen dataset using the Weighted Averaging Partial Least Squares (WAPLS). Significant relationships were detected between pollen assemblages and  $P_{\text{ann}}$  ( $R^2 = 0.81$ , RMSEP = 56.1 mm, maximum bias = 65.6 mm).  
240 Our results indicate that the regional pollen dataset can provide useful and reliable quantitative estimates of past precipitation change in the central and western TP. The pollen-derived transfer function was tested for a pollen record on the central TP, which is the first quantitative paleo-precipitation record in the Indian summer monsoon margin.

Most of our lake sites are located in extremely remote areas with difficult access. The pollen data from these localities can fill the geographical gap left by other published modern pollen datasets and make the samples evenly distributed in the combined pollen dataset. Apart from its use for quantitative precipitation reconstructions in the central and western TP, our dataset can also be combined with other pollen datasets to improve the reliability of quantitative climate reconstructions across the entire TP.  
245

**Author contributions.** LZ designed the study. QM, JJ, JW, YW, and LH collected the samples. QM made the pollen extraction and identification, and drafted the manuscript. JJ, JW, YW, LH and TH revised the manuscript.

250 **Competing interests.** The contact author has declared that none of the authors has any competing interests.

**Disclaimer.** Publisher's note: Copernicus Publications remains neutral with regard to jurisdictional claims in published maps and institutional affiliations.



**Acknowledgements.** We thank all colleagues and students in the field for their help with sampling. We would like to thank Prof. Qinghai Xu, Prof. Lingyu Tang and Dr. Xinmiao Lü for their help with sample treatment and pollen identification. Climate data were provided by the National Tibetan Plateau Data Center.

**Financial support.** This research has been supported by the National Natural Science Foundation of China (41831177, 42272223), the Second Tibetan Plateau Scientific Expedition and Research (STEP) (2019QZKK0202), and the Innovation Program for Young Scholars of TPESER (TPESER-QNCX2022ZD-01).

## References

- Birks, H. J. B., Line, J. M., Juggins, S., Stevenson, A. C., ter Braak, C. J. F.: Diatoms and pH reconstruction, *Philos. Trans. R. Soc. B*, 327, 263–278., doi:10.1098/rstb.1990.0062, 1990.
- 265 Birks, H. J. B.: Numerical tools in palaeolimnology—progress, potentialities, and problems, *J. Paleolimnol.*, 20, 307–332, doi:10.1023/A:1008038808690, 1998.
- Birks, H. J. B., Heiri, O., Seppä H., Björne, A. E.: Strengths and weaknesses of quantitative climate reconstructions based on late-Quaternary biological proxies, *Open Ecol. J.*, 3, 68–110, doi:10.2174/1874213001003020068, 2010.
- 270 Cao, X., Tian, F., Li, K., Ni, J., Yu, X., Liu, L., Wang, N.: Lake surface sediment pollen dataset for the alpine meadow vegetation type from the eastern Tibetan Plateau and its potential in past climate reconstructions, *Earth Syst. Sci. Data*, 13, 3525–3537, doi:10.5194/essd-13-3525-2021, 2021.
- Fægri, K., Iversen, J.: *Textbook of pollen analysis*, Munksgaard, Copenhagen, 1975.
- He, J., Yang, K., Tang, W., Lu, H., Qin, J., Chen, Y., Li, X.: The first high-resolution meteorological forcing dataset for land process studies over China, *Sci. Data*, 7, 25, doi:10.1038/s41597-020-0369-y, 2020.
- 275 Herzschuh, U., Birks, H. J. B., Mischke, S., Zhang, C., Böhner, J.: A modern pollen-climate calibration set based on lake sediments from the Tibetan Plateau and its application to a late Quaternary pollen record from the Qilian Mountains, *J. Biogeogr.*, 37, 752–766, doi:10.1111/j.1365-2699.2009.02245.x, 2010.
- Hill, M. O.: Diversity and evenness: A unifying notation and its consequences, *Ecology*, 54, 427–432, doi:10.2307/1934352, 1973.
- 280 Hou, X.: *Vegetation Atlas of China*, Science Press, Beijing, 2001.
- Institute of Geography: *Map of the Qinghai-Tibetan Plateau*, Science Press, Beijing, 1990.
- ITCAS (Investigation Team of Chinese Academy of Science): *Vegetation in Tibetan Plateau*, Science Press, Beijing, 1988.
- Juggins, S.: *User Guide: C2, software for ecological and palaeoecological data analysis and visualization user guide version 1.3.*, Department of Geography University of Newcastle, Newcastle upon Tyne, 69 pp, 2003.
- 285 Lu, H., Wu, N., Liu, K., Zhu, L., Yang, X., Yao, T., Wang, L., Li, Q., Liu, X., Shen, C., Li, X., Tong, G., Jiang, H.: Modern pollen distributions in Qinghai-Tibetan Plateau and the development of transfer functions for reconstructing Holocene environmental changes, *Quat. Sci. Rev.*, 30, 947–966, doi:10.1016/j.quascirev.2011.01.008, 2011.



- Ma, Q., Zhu, L., Lu, X., Wang, Y., Guo, Y., Wang, J., Ju, J., Peng, P., Tang, L.: Modern pollen assemblages from surface lake sediments and their environmental implications on the southwestern Tibetan Plateau, *Boreas*, 46, 242–253, doi:10.1111/bor.12201, 2017.
- Ma, Q., Zhu, L., Lü, X., Wang, J., Ju, J., Kasper, T., Daut, G., Haberzettl, T.: Late glacial and Holocene vegetation and climate variations at Lake Tangra Yumco, central Tibetan Plateau, *Global Planet. Change*, 174, 16–25, doi:10.1016/j.gloplacha.2019.01.004, 2019.
- Ma, Q., Zhu, L., Wang, J., Ju, J., Wang, Y., Lü, X., Kasper, T., Haberzettl, T.: Late Holocene vegetation responses to climate change and human impact on the central Tibetan Plateau, *Sci. Total Environ.*, 708, 135370, doi:10.1016/j.scitotenv.2019.135370, 2020.
- Nakagawa, T., Tarasov P. E., Nishida, K., Gotanda, K., Yasuda, Y.: Quantitative pollen-based climate reconstruction in central Japan: application to surface and Late Quaternary spectra, *Quat. Sci. Rev.*, 21, 2099–2113, doi:10.1016/S0277-3791(02)00014-8, 2002.
- Overpeck, J. T., Webb III, T., Prentice, I. C.: Quantitative interpretation of fossil pollen spectra: Dissimilarity coefficients and the method of modern analogs, *Quat. Res.*, 23, 87–108, doi:10.1016/0033-5894(85)90074-2, 1985.
- Prentice, I. C.: Multidimensional scaling as a research tool in Quaternary palynology: a review of theory and methods, *Rev. Palaeobot. Palynol.*, 31, 71–104, doi:10.1016/0034-6667(80)90023-8, 1980.
- R Core Team: R, A language and environment for statistical computing, R Foundation for Statistical Computing, Vienna, 2023.
- Seppä H., Birks, H. J. B., Odland, A., Poska, A., Veski, S.: A modern pollen–climate calibration set from northern Europe: developing and testing a tool for palaeoclimatological reconstructions, *J. Biogeogr.*, 31, 251–267, doi:10.1111/j.1365-2699.2004.00923.x, 2004.
- Shen, C., Liu, K., Tang, L., Overpeck, J. T.: Quantitative relationships between modern pollen rain and climate in the Tibetan Plateau, *Rev. Palaeobot. Palynol.*, 140, 61–77, doi:10.1016/j.revpalbo.2006.03.001, 2006.
- Tang, L., Mao, L., Shu, J., Li, C., Shen, C., Zhou, Z.: Atlas of Quaternary pollen and spores in China, Science Press, Beijing, 2017.
- Telford, R. J., Birks, H. J. B.: A novel method for assessing the statistical significance of quantitative reconstructions inferred from biotic assemblages, *Quat. Sci. Rev.*, 30, 1272–1278, doi:10.1016/j.quascirev.2011.03.002, 2011.
- Telford, R. J., Trachsel, M.: PalaeoSig: Significance tests for palaeoenvironmental reconstructions, version 2.1-3, available at: <http://cran.r-project.org/web/packages/palaeoSig/index.html>, 2023.
- ter Braak, C. J. F., Juggins S.: Weighted averaging partial least squares regression (WA-PLS): an improved method for reconstructing environmental variables from species assemblages, *Hydrobiologia*, 269, 485–502, doi:10.1007/BF00028046, 1993.
- ter Braak, C. J. F., Smilauer, P.: CANOCO reference manual and user’s guide: software for ordination (version 5), Microcomputer Power Ithaca, New York, 2012.



- Wang, F., Qian, N., Zhang, Y., Yang, H.: Pollen flora of China, Science Press, Beijing, 1995.
- Wang, M., Tian, Q., Li, X., Liang, J., He, Y., Hou, J.: TEX<sub>86</sub> as a potential proxy of lake water pH in the Tibetan Plateau, *Palaeogeogr. Palaeoclimatol. Palaeoecol.*, 538, 109381, doi:10.1016/j.palaeo.2019.109381, 2020.
- 325 Wilmshurst, J. M., McGlone, M. S.: Origin of pollen and spores in surface lake sediments: comparison of modern palynomorph assemblages in moss cushions, surface soils and surface lake sediments, *Rev. Palaeobot. Palynol.*, 136, 1–15, doi:10.1016/j.revpalbo.2005.03.007, 2005.
- Yao, T., Masson-Delmotte, V., Gao, J., Yu, W., Yang, X., Risi, C., Sturm, C., Werner, M., Zhao, H., He, Y., Ren, W., Tian, L., Shi, C., Hou, S.: A review of climatic controls on  $\delta^{18}\text{O}$  in precipitation over the Tibetan Plateau: observations and simulations, *Rev. Geophys.*, 51, 525–548, doi:10.1002/rog.20023, 2013.
- 330 Zhang, E., Chang, J., Shulmeister, J., Langdon, P., Sun, W., Cao, Y., Yang, X., Shen, J.: Summer temperature fluctuations in Southwestern China during the end of the LGM and the last deglaciation, *Earth Planet. Sc. Lett.*, 509, 78–87, doi:10.1016/j.epsl.2018.12.024, 2019.
- Zhao, Y., Xu, Q., Huang, X., Guo, X., Tao, S.: Differences of modern pollen assemblages from lake sediments and surface soils in arid and semi-arid China and their significance for pollen-based quantitative climate reconstruction, *Rev. Palaeobot. Palynol.*, 156, 519–524, doi:10.1016/j.revpalbo.2009.05.001, 2009.
- 335